WP-2613 SEED FINAL REPORT:

Optical Diagnostics for Evaluating Emissions from Metal-Based Energetic Formulations

Naval Air Warfare Center Weapons Division
Lead PI: Claresta Dennis

12 December 2017

REPORT DOCUMENTATION PAGE

Form Approved
OMB No. 0704-0188

1. REPORT DATE *(DD-MM-YYYY)*	**2. REPORT TYPE**	**3. DATES COVERED** *(From - To)*
12-12-2017	SERDP Final Report	June 2016 - May 2017

4. TITLE AND SUBTITLE

Optical Diagnostics for Evaluating Emissions from Metal-Based Energetic Formulations

5a. CONTRACT NUMBER

5b. GRANT NUMBER
16 WPSEED01-007 / WP-2613

5c. PROGRAM ELEMENT NUMBER

6. AUTHOR(S)

CN Dennis
TT Tran-Ngo

5d. PROJECT NUMBER
WP-2613

5e. TASK NUMBER

5f. WORK UNIT NUMBER

7. PERFORMING ORGANIZATION NAME(S) AND ADDRESS(ES)

Naval Air Warfare Center Weapons Division
1 Administration Circle
China Lake, CA 93555

8. PERFORMING ORGANIZATION REPORT NUMBER

WP-2613

9. SPONSORING / MONITORING AGENCY NAME(S) AND ADDRESS(ES)

Strategic Environmental Research and Development Program
4800 Mark Center Drive, Suite 17D03
Alexandria, VA 22350-3605

10. SPONSOR/MONITOR'S ACRONYM(S)

SERDP

11. SPONSOR/MONITOR'S REPORT NUMBER(S)

WP-2613

12. DISTRIBUTION / AVAILABILITY STATEMENT

Approved for Public Release, Distribution is Unlimited

13. SUPPLEMENTARY NOTES

14. ABSTRACT

The objective of this project was to assess the use of three different optical diagnostic techniques for the standoff detection of hazardous combustion products produced from the reaction of energetic and pyrotechnic formulations. By performing laboratory scale testing for proof-of-concept, useful data will be obtained for comparison with thermochemical calculations and insight towards the miniaturization and simplification of the diagnostic techniques for eventual application in a field-ready system.

This optical methodology for emissions characterization will enable standoff detection of hazardous combustion products, providing data regarding metal species and soot generated as a function of time. The techniques used can be readily integrated into a ruggedized field-use system that is mobile and compact. Measurements by such a system would allow the Department of Defense to model and predict potential range contamination, occupational exposure levels on ranges, and the migration of airborne contaminants. This also may serve as a methodology to assess new technologies employed for reducing the long-term health effects for DOD firing ranges.

15. SUBJECT TERMS

optical diagnostics, incendiary filler, gun powder, spectroscopy, fiber optic, emissions, light extinction, laser induced incandescence

16. SECURITY CLASSIFICATION OF:			**17. LIMITATION OF ABSTRACT**	**18. NUMBER OF PAGES**	**19a. NAME OF RESPONSIBLE PERSON**
a. REPORT	**b. ABSTRACT**	**c. THIS PAGE**			Claresta Dennis
Unclassified	Unclassified	Unclassified	Unclassified	33	**19b. TELEPHONE NUMBER** *(include area code)* 760-939-4050

Table of Contents

List of Tables

List of Figures

List of Acronyms

CCD	charge coupled device
CMOS	complementary metal oxide semiconductor
CV	constant volume
CW	continuous wave
DOD	Department of Defense
iCCD	intensified charge coupled device
LIBS	laser induced breakdown spectroscopy
LII	laser induced incandescence
SEED	SERDP exploratory development
SON	statement of need
NC	nitrocellulose
NG	nitroglycerine
UV-VIS	ultraviolet-visible

Keywords

optical diagnostics, nonintrusive, lasers, incendiary filler, gun powder, spectroscopy, fiber optic, emissions, light extinction, laser induced incandescence

Abstract

Objectives

The objective of this project was to assess the use of three different optical diagnostic techniques for the standoff detection of hazardous combustion products produced from the reaction of energetic and pyrotechnic formulations. By performing laboratory scale testing for proof-of-concept, useful data will be obtained for comparison with thermochemical calculations and insight towards the miniaturization and simplification of the diagnostic techniques for eventual application in a field-ready system.

Technical Approach

A 4-Liter combustion chamber was instrumented for the simultaneous application of three optical diagnostic techniques: UV/VIS spectroscopy, light extinction, and laser induced incandescence. The techniques were selected because they are optical, non-intrusive, and can be used to characterize the atomic and molecular species, soot, and condensed phase particles present in the combustion products of metal-based energetic and pyrotechnic formulations. High-speed UV-VIS emission spectroscopy performed using a spectrometer-coupled streak camera was used to assess the production and lifetimes of metal species of interest during the reactions. Light extinction measurements provide a qualitative assessment of soot production as a function of time. Laser induced incandescence allows the characterization of particle size distribution of metals/soot over time during a combustion event.

Samples of $BKNO_3$, IM-23, IM-68, and Hercules Red Dot were initiated at atmospheric pressure using an electric match. An ultrafast laser system was used to provide the input source for both light extinction and laser induced incandescence measurements. For light extinction measurements an integrating sphere and photodiode were used to detect the transmitted laser intensity through the reaction path. Sheet forming optics were used for 2-dimensional LII measurements and the signal was detected in the direction perpendicular to the laser sheet using an imaging detector and laser line filter. A fiber optic cable and collimator enabled signal collection for the spectroscopic measurements. In addition to experimental work, the thermochemical code CHEETAH was used to determine the combustion products and temperature of the energetic material reactions.

Results

Spectroscopic measurements were consistent with CHEETAH calculations of combustion products. The emission spectrum obtained from $BKNO_3$ contains atomic lines of potassium at 766.4 and 769.8 nm as expected. Measurements from IM-23 show atomic lines of magnesium and potassium. The emission spectrum from IM-68 shows features from diatomic oxygen, nitrogen, magnesium, and barium. Measurements of the Red Dot reaction show nitrogen and cyanide. In addition spectra obtained from IM-23, IM-68, and Red Dot all have contamination from sodium which is evident by the emission line at 588 nm. Sodium is a common contaminant in energetic materials.

Light extinction measurements and high speed video recording of the reactions showed materials with more condensed phase products caused greater attenuation of the laser signal. Results showed that the fastest reaction is complete in ~0.02 seconds, indicating a data acquisition rate of 500 Hz should be sufficient for future measurements.

For the laboratory proof-of-concept LII measurements the detector repetition rate was too slow to resolve the signal. The 5 kHz pulsed laser system and speed of the energetic material reactions caused difficulty for adequate signal detection to record the LII signal decay and determine particle size. However, it was clear from the recorded images that additional information is obtained when compared to the standard high speed video images. In the LII images fine smoke particles are visible which are otherwise not detectable by the standard high speed camera. Based on the laser source parameters and detection scheme for this experimental setup we can visualize fine smoke particles as small as 0.3 μm in diameter.

Benefits

This optical methodology for emissions characterization will enable standoff detection of hazardous combustion products, providing data regarding metal species and soot generated as a function of time. The techniques used can be readily integrated into a ruggedized field-use system that is mobile and compact. Measurements by such a system would allow the Department of Defense to model and predict potential range contamination, occupational exposure levels on ranges, and the migration of airborne contaminants. This also may serve as a methodology to assess new technologies employed for reducing the long-term health effects for DOD firing ranges.

Objective

The goal of this project was to assess the use of three different optical diagnostic techniques for the standoff detection of hazardous combustion products produced from the reaction of energetic and pyrotechnic formulations as solicited in the SEED SON. The combination of experimental techniques was selected based on the feasibility of future technology transfer into a rugged field-able type system. The objective was to perform laboratory scale testing for proof of concept to obtain useful data for comparison with thermochemical calculations and insight towards the miniaturization and simplification of the diagnostic techniques for eventual application in a field-ready system.

The diagnostic techniques selected were UV-VIS spectroscopy, light extinction, and laser induced incandescence for the simultaneous measurement of combustion product species, soot generation, and condensed phase particle size and volume fraction. This would enable assessment of the airborne metals and harmful chemicals generated during energetic and pyrotechnic combustion events. By determining which atomic and molecular species are important and under what time scales they are produced, a focused approach to properly transition high fidelity lab-based techniques to a field-ready compact fiber optic-based system is possible. Development of such a mobile and compact system, as an extensive follow-on project, may be used in the field to assess new technologies employed for reducing the long-term health effects associated with airborne metal emissions.

Background

Increased concern for the long-term health effects associated with lead exposure and inhalation of particulates has highlighted the need for methods of characterizing metal and other hazardous combustion products released during the military's use of lead-based primary explosives and metal-based pyrotechnic formulations. The toxicity of heavy metals is associated with their bioavailability and solubility[1]. Unfortunately, in contrast to the naturally occurring minerals, the majority of metal compounds set free from pyrotechnics and explosives are water soluble and bioavailable[2]. For example, studies have found heavy metal contamination in snow following New Year's Eve pyrotechnics[3].

In order to properly quantify the hazards produced, species identification of the combustion products is required. Non-invasive experimental methods are ideal for emissions characterization as thermodynamic models for non-ideal explosives often contain inaccuracies. In addition, optical methods can probe the reaction zone at a standoff distance as to not disturb the reaction's propagation and subsequent chemistry. Emission spectroscopy is widely employed for obtaining atomic and molecular spectra generated during combustion reactions. Timescales under which the species appear is also important for reaction kinetics as well as understanding how to mitigate heavy metal exposure. High-speed spectroscopy may be performed using a spectrometer coupled with a streak camera. Experiments have been performed previously obtaining emission spectra from lead azide and silver azide using a streak camera, though their spectral resolution was poor and many of the emission lines were left unidentified[4,5]. Grisch has shown that the detonation of lead azide yields lead atoms and triplet state N_2 molecules and collisional energy transfer preferentially populates the $^3P_1$ state of lead leading to enhancement of the atomic emission line at 722.9 nm[6]. This emission line enhanced specifically during the reaction of lead azide is a good starting point for UV-VIS spectroscopy studies. The magnitude of emission line intensity is proportional to the emitting species number density. A systematic approach of increasing sample size should produce the relative lead concentration present during the combustion reaction.

In addition to the toxicity of bioavailable heavy metals, inhalation hazards exist from the soot and superfine particulates generated during the testing of primary explosives. Fine, metal-rich particles can have toxic effects on human health. Crespo, *et al.* sampled the aerosol cloud produced by a large fireworks display, consisting of thousands of firecrackers in Spain[7]. They found copper, sulfur, potassium, and calcium with particle size distributions centered between 0.1 to 10 microns in diameter. Typically, particle size distributions are obtained by large volume air sampling or by collecting residues for analysis. Both of these methods are time consuming and cannot be performed *in-situ* at fast data sampling rates for munitions analysis.

To access the potential health hazards present with munitions and ordinance firing, the community needs soot volume fraction, particle size measurements and emissions speciation information with high temporal resolution. The measurements should be non-intrusive as to not disturb the flow-field and utilize techniques rugged enough for integration into a field-ready device.

Materials and Methods

All experiments were performed remotely in a combustion chamber with optical access. A photograph of the chamber is shown in Figure 1. The chamber is approximately 4 L in volume and has 5 ports for instrumentation or optical access. The chamber was engineered to contain 2000 psi pressure, with a safety factor of 4, when steel platens are installed in all ports. For optical access the platens are removed and replaced with windows of the appropriate material, spectral transmission, and pressure rating. For this work the optical access windows used were 0.125" thick sapphire. When the sapphire window is installed the maximum pressure the vessel can contain, with a safety factor of 4, is 408 psi. The top of the chamber is removable for sample insertion and ease of cleaning. The chamber also has a dedicated opening at the top and bottom for pressurized air intake and exhaust.

Figure 1: Photograph of the 4L combustion chamber.

The chamber was instrumented for simultaneous application of the three experimental diagnostic techniques: UV/VIS spectroscopy, light extinction, and laser induced incandescence. A schematic of the chamber diagnostics layout top and side views are shown in Figure 2.

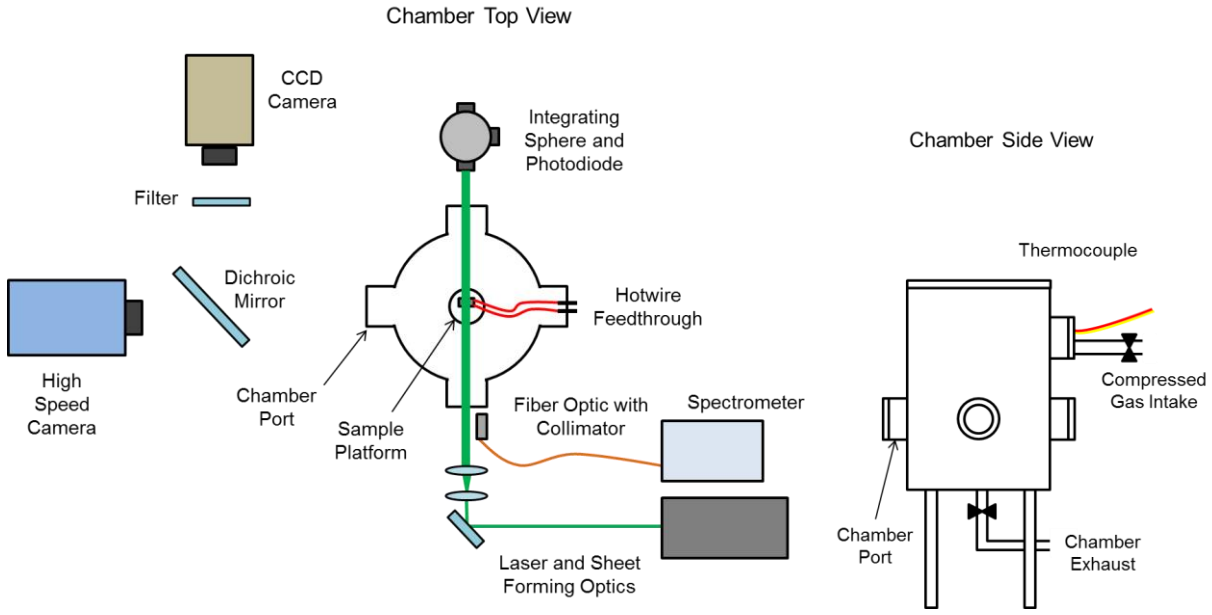

Figure 2: Schematic of the medium combustion chamber instrumentation setup.

Data collection for the various experimental techniques was synchronized using a digital delay generator (Stanford Research Systems DG535) for precise timing and triggering. Photodiode, ignitor voltage, and ignitor current data was collected using a high-speed data acquisition system (HBM Gen5i DAQ). To ignite the energetic material samples an electronic match or 'e-match' was used. The e-match consists of a thin nichrome hotwire dipped in pyrogen. A power supply (BK Precision 9152 30V/18A DC) provided the 9 V required for initiating the e-match. In addition to the diagnostic techniques, each test's reaction event was recorded using a high speed camera (Photron SA5 with Nikon Micro-Nikkor 105mm 1:2.8 camera lens). For some experiments a thermocouple rake was insetered over the sample holder in order to measure the flame temperature. A schematic indicating the thermocouple locations is shown in Figure 3. Type-K thermocouples were used.

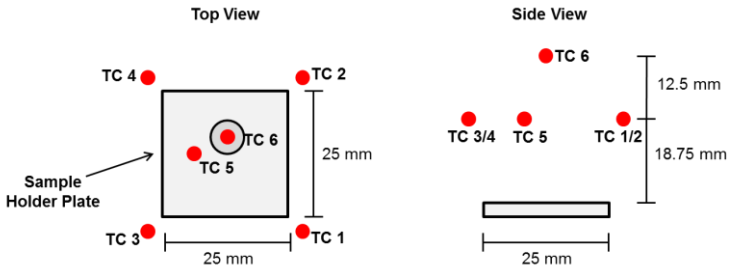

Figure 3: Schematic of thermocouple locations with respect to the sample holder.

UV-VIS Emission Spectroscopy

During a combustion/deflagration event, the thermal energy present excites gas phase atoms to excited electronic states, which then emit light when they return to their ground electronic state. The wavelengths of emitted light are unique characteristics used for elemental

identification while the intensity of the emitted light produces a signal proportional to the number of atoms/molecules of the element present in the sampling volume. Performing high-speed UV-VIS emission spectroscopy allows us to characterize the products of combustion produced during a combustion event. For these measurements typically, a set of optics collects the light from the flame emission and a grating disperses the light that impinges on a detector. The experimental setup used for this work is shown in Figure 4.

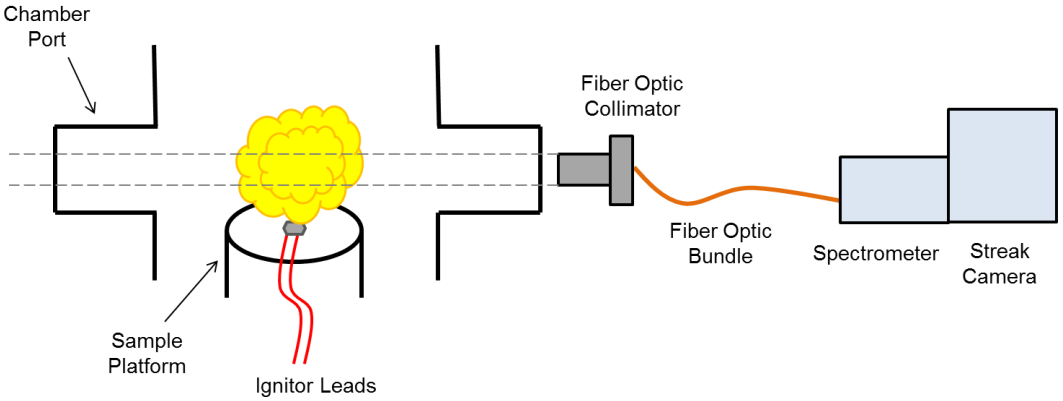

Figure 4: Schematic of UV/VIS spectroscopy experimental setup.

In order to efficiently gather light from the reactions a fiber optic collimator, Thor Labs RC12SMA-P01, was used to collect over a 12 mm diameter collimated area and focus the light into a fiber optic. A custom fiber optic bundle suitable for spectrometer use (Fiber Optic Systems 19 core FDP200220245 .22NA fiber) was used to transmit the light from the collimator to the spectrometer. On one end of the bundle fibers are arranged in a circular grouping and on the other end the fibers are fixed into a single column which is then aligned to the spectrometer's slit. A streak camera (Hamamatsu C5680 and OrcaR2) coupled to a spectrometer (PIACTON SpectraPro SP2300i) was used to obtain measurements with high temporal resolution.

In order to assess the application of UV/VIS spectroscopy in a future portable system, a compact fiber optic based spectrometer (Ocean Optics HR4000CG-UV-NIR) was also used to collect data.

Light Extinction

The light extinction technique measures the baseline light transmitted intensity from a blank sample volume and the sample light transmitted intensity from soot filled sample volume. Bouguer's Law relates the ratio of the baseline and the sample light transmitted intensity to the soot's volume fraction in a sample[8]. The biggest challenge is distinguishing the input signal from the luminous reaction emission. The current method uses three different means to distinguish the input signal from flame emission: modulation, polarization, and dispersion. Modulation of the input light at a known frequency allows the input signal to be discriminated from the sample luminosity. Polarization of the input light at a specific orientation further discriminate the input signal from the sample. Finally, dispersion is wavelength discrimination[9], which uses a known wavelength profile for the input light and measuring at the same wavelength profile from the sample. Light extinction measurements provide a qualitative measure of the soot formation over time during an energetic/pyrotechnic combustion reaction.

The experimental setup used for this work is shown in Figure 5. A femtosecond laser system (Coherent Legend Elite Duo Femto) provided the input light source. This laser produces 100 fs duration laser pulses at a repetition rate of 5 kHz and 800 nm center wavelength. The beam is transmitted through the combustion chamber optical access windows and the center of the reaction zone. After exiting on the opposite side of the chamber, the beam is collected by an integrating sphere (LabSphere 3P-GPS-040-SF). The transmitted beam intensity is detected using a silicon photodiode (ThorLabs Mounted Si photodiode SM05PD2B).

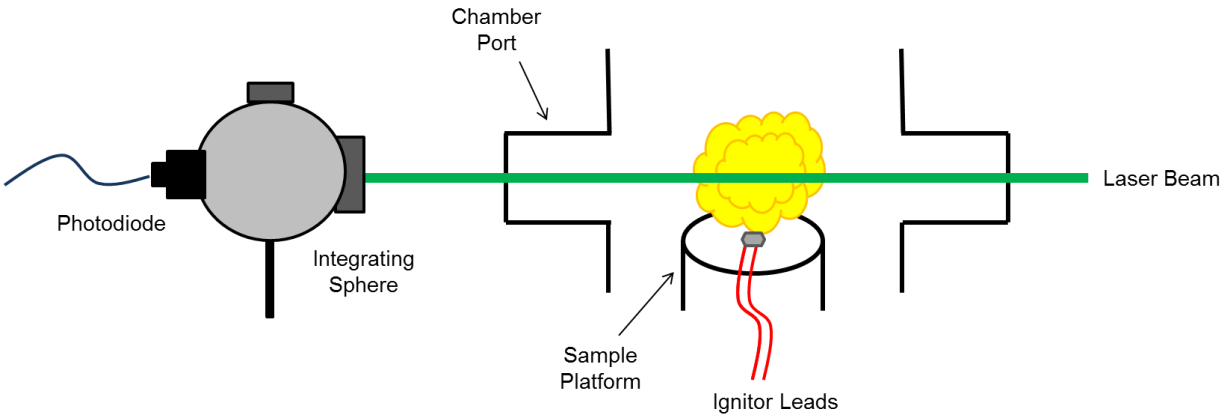

Figure 5: Schematic of experimental setup for light extinction measurements.

Laser Induced Incandescence

The LII technique involves exposing a volume of gas containing refractory particles to a focused pulse of high-intensity laser light. The particles absorb the laser energy and heat to temperatures far above the surrounding gas. At these elevated temperatures (about 4000-4500 K in the case of soot) the particles incandesce strongly throughout the visible and near infrared region of the spectrum[10]. The radiative emission is shifted to higher frequency allowing the LII signal to be isolated from natural flame emission. The LII signal magnitude can be correlated with the volume fraction of particles in the detection region. The transient cooling process, which determines the decay rate of the signal, is dependent upon the diameter of the particle. Therefore, the decay rate correlates to the particle size[11]. Due to the rapid time scales, spatial resolution, and dynamic range, LII is well suited as an optical diagnostic to measure soot volume fraction in turbulent and time varying combustion devices[12].

Little work has been done to determine the optimum laser pulse duration used to initiate the LII process. The majority of the studies reported are based on 7 to 10-ns pulse duration with recent work from Ditaranto, *et.al*. using much longer duration pulses generated from a CW laser[13]. The present work utilizes an ultrafast laser system, producing laser pulses with 100 fs duration. The shorter pulse duration should provide higher peak laser intensity and more efficiently heat the soot/condensed phase metallic species present. Using the LII technique enables characterization of the particle size distribution of combustion products over time during the reaction. A short duration pulsed laser is inherently broadband. The additional bandwidth provided by an ultrafast laser system should be advantageous in providing a better LII signal as shown in Figure 6. The purple and blue lines in the plot show the broadband and narrowband LII signal, respectively. The black line is the laser scattering signal and the dotted yellow line represents the laser-particle interaction time.

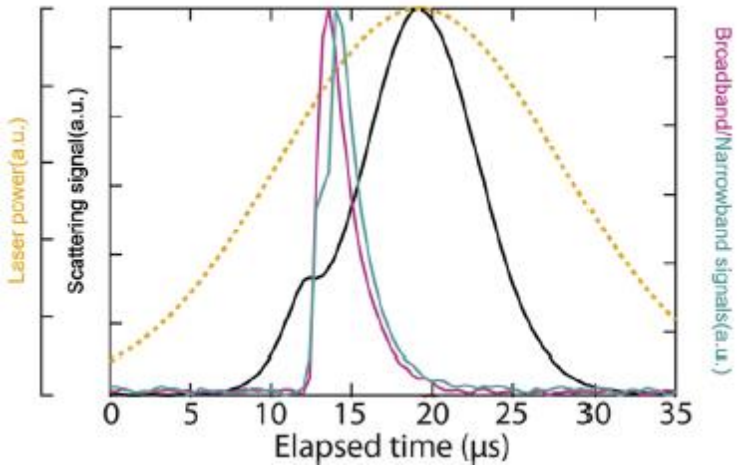

Figure 6: LII and laser scattering profiles from a particle, Ref. 16.

The experimental setup used for this work is shown in Figure 7. A femtosecond laser system (Coherent Legend Elite Duo Femto) provided the excitation light source. The beam was transformed into a sheet 25 mm tall and ~250 μm thick prior to transmission through the combustion chamber optical access windows. An intensified charge coupled device (PIMAX 3 1024i iCCD with Unigen2 coating with Nikon UV-Nikkor 105mm 1:4.5 camera lens) was used to detect the LII signal through an optical access window perpendicular to the laser sheet.

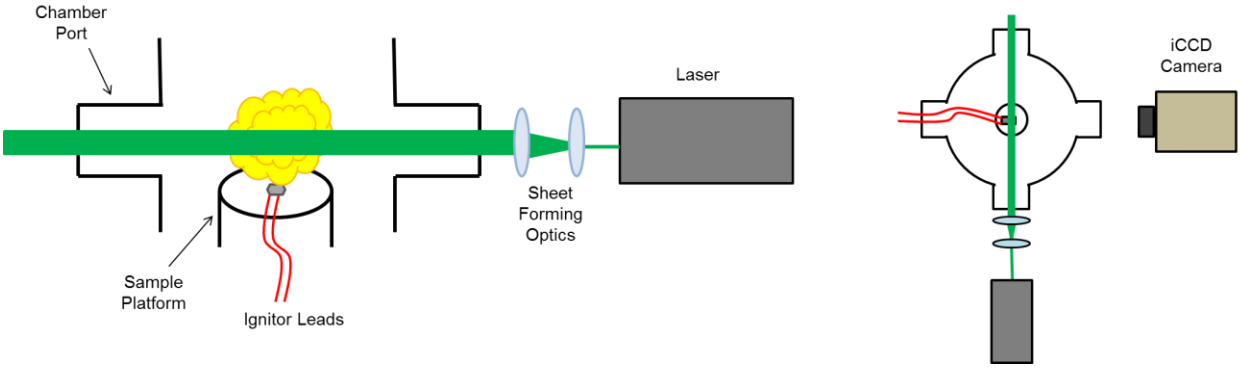

Figure 7: Schematic of experimental setup for laser induced incandescence measurements.

Table 1: Description of energetic materials tested.

Material	Composition	Form	Hazard Class	Quantity Per Test	Additional Information
Boron potassium nitrate	$BKNO_3$	Loose powder	1.3	20-50 mg	Burns with intense heat and gives off toxic fumes. It may explode if confined while burning.

Material	Composition	Form	Hazard Class	Quantity Per Test	Additional Information
Navy IM-23 (also known as RS-41, nose fill for PGU-28A/B)	49% Mg/Al alloy 49% $KClO_4$ 2% calcium resinate	Incendiary filler	1.1D	20-50 mg	Burns rapidly with intense heat.
Navy IM-68 (also known as RS-40, body fill for PGU-28A/B)	48% Mg/Al alloy 25% NH_4NO_3 25% $Ba(NO_3)_2$ 2% calcium resinate	Incendiary filler	1.1D	20-50 mg	Burns rapidly with intense heat.
Hercules Red Dot (double based gun powder)	20% nitroglycerin 80% nitrocellulose	Granules	1.3	20-50 mg	Reacts violently with many chemicals causing fire and explosion hazard. Material is sensitive to friction, shock, impact, and electrostatic discharge.

Energetic material samples were selected based on fleet-use significance and material availability. Heavy metal containing samples were determined prohibitive for this project due to cost and schedule impacts resulting from safety requirements determined by Industrial Health and Occupational Health and Safety inspection prior to testing. Testing the M52A3B1 electric primer, containing lead, copper, and antimony sulfide, was not pursued due to safety concerns unloading powder from primer caps.

Results and Discussion

The goal of this project was to assess the use of three different optical diagnostic techniques for the standoff detection of hazardous combustion products produced from the reaction of energetic and pyrotechnic formulations. Laboratory scale testing has been performed for proof-of-concept to obtain data for comparison with thermochemical calculations and insight towards the miniaturization and simplification of the diagnostic techniques for eventual application in a field-ready system. Each experimental technique is optical line of sight, non-intrusive, and can be applied using fiber optics.

UV-VIS Emission Spectroscopy

For spectroscopy data collection, first a high temporal resolution streak camera detector was used. This detector collects spectral information as a function of time. Experiments were performed with a 1.0 ms streak duration and 50 nm spectral resolution. Streak camera results were compared with corresponding high speed camera images of the flame front. Figure 8 shows several streak images from the IM-68 reaction. The emission profiles do not vary significantly as a function of time.

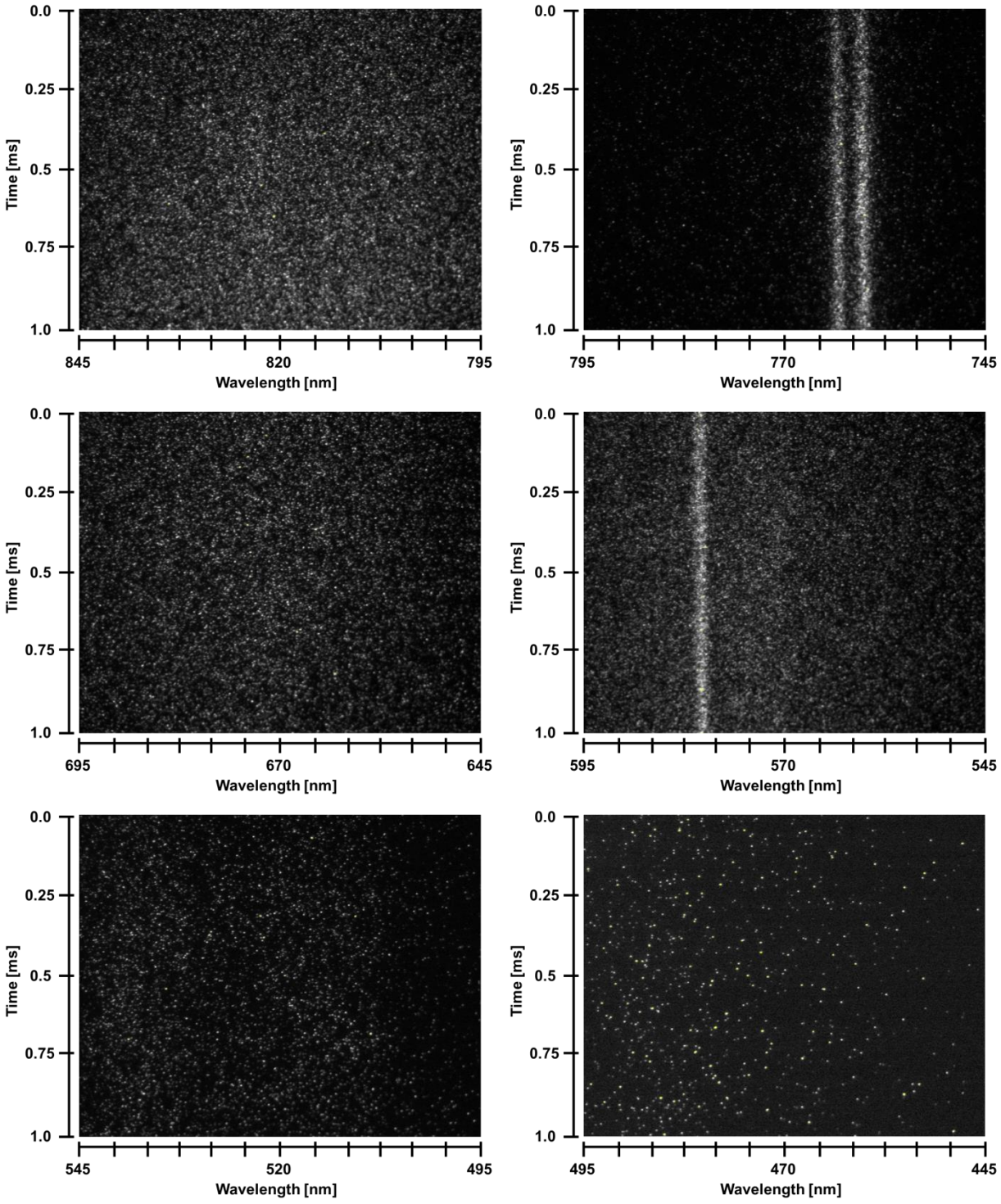

Figure 8: Streak emission spectra from IM-68 reaction.

For application in a field-ready system the high temporal resolution spectra obtained with the streak camera is not practical. The streak cameras commercially available today are costly and meant to be used in a stable, vibration free, temperature controlled laboratory environment. Experimental results do not indicate a need for high speed measurements, evidence of short lived

molecular species which may cause respiratory harm to the warfighter was not observed. The streak camera coupled spectrometer system was then replaced with a portable fiber optic based spectrometer. Resulting emission spectra are shown in Figure 9 through Figure 13. The dashed outline indicates the light extinction/LII laser output which has been removed from the dataset.

The emission spectrum from $BKNO_3$ is shown in Figure 9 and Figure 10. Measurements show atomic lines of K at 766.4 and 769.8 nm as expected. In addition, weak features of BO_2 are seen at 518 and 547 nm. The green hue characteristic of boron oxide emission is clearly visible in the high speed video series. This light was inefficiently collected by the fiber optic placement.

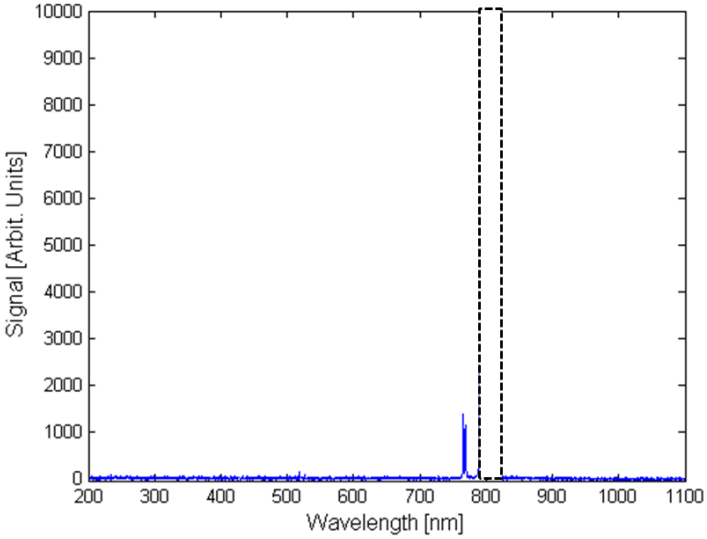

Figure 9: Emission spectra from $BKNO_3$ reaction recorded using Ocean Optics spectrometer.

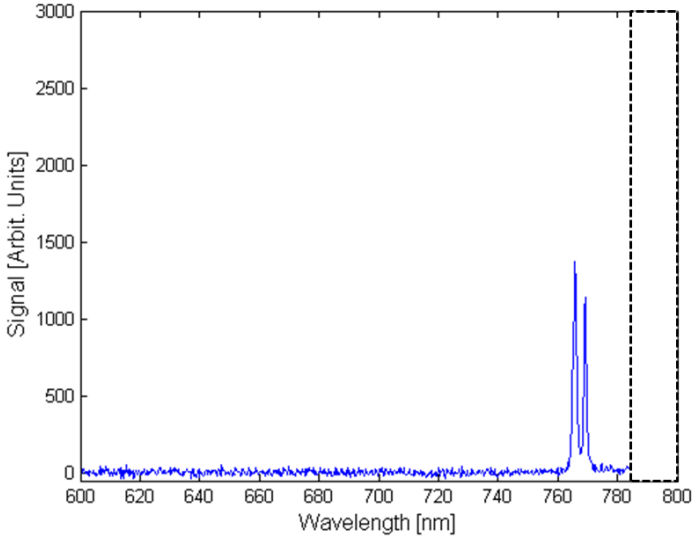

Figure 10: Emission spectra from $BKNO_3$ reaction recorded using Ocean Optics spectrometer from 600 to 800 nm.

The emission spectrum from IM-23 is shown in Figure 11. Measurements show atomic lines of Mg and K as expected. Contamination from sodium is evident by the spectral line at 588 nm. Sodium is a common contaminant in energetic materials.

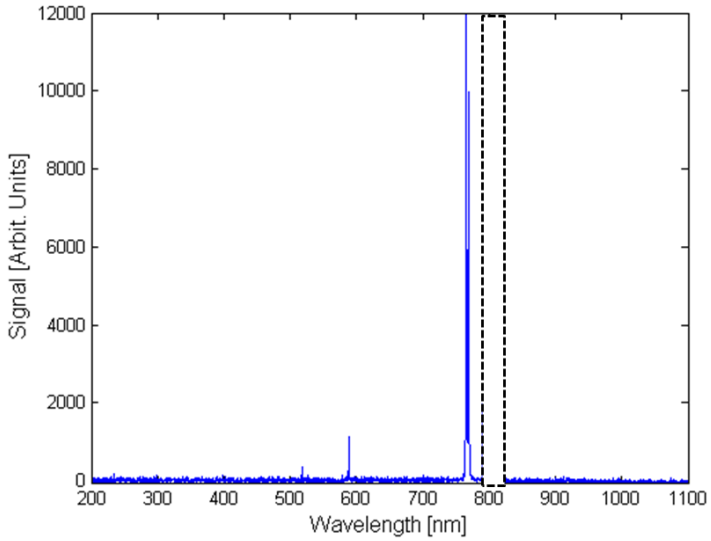

Figure 11: Emission spectra from IM-23 reaction recorded using Ocean Optics spectrometer.

The emission spectrum from IM-68 is shown in Figure 12. Measurements show features from O_2, N_2, Mg, and Ba as expected, in addition evidence of the contaminants sodium and calcium. The broadband features are characteristic of gas phase molecular species.

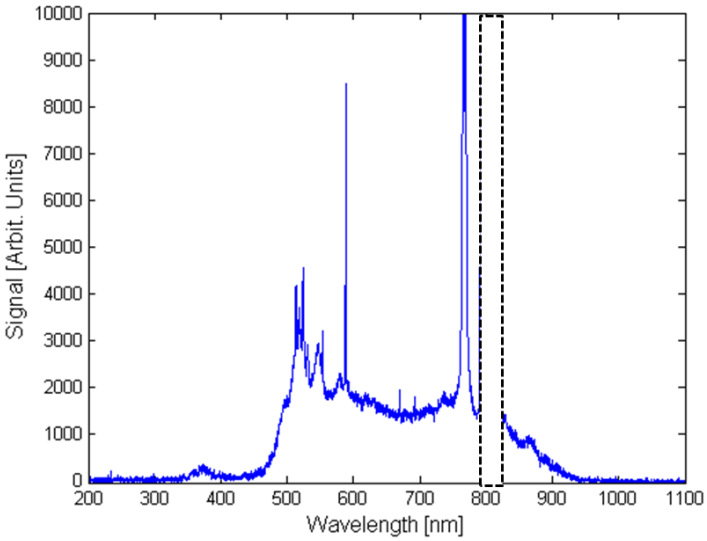

Figure 12: Emission spectra from IM-68 reaction recorded using Ocean Optics spectrometer.

The emission spectrum from Red Dot gun powder is shown in Figure 13. Measurements show features from N_2, CN, and evidence of the contaminants sodium and silicon.

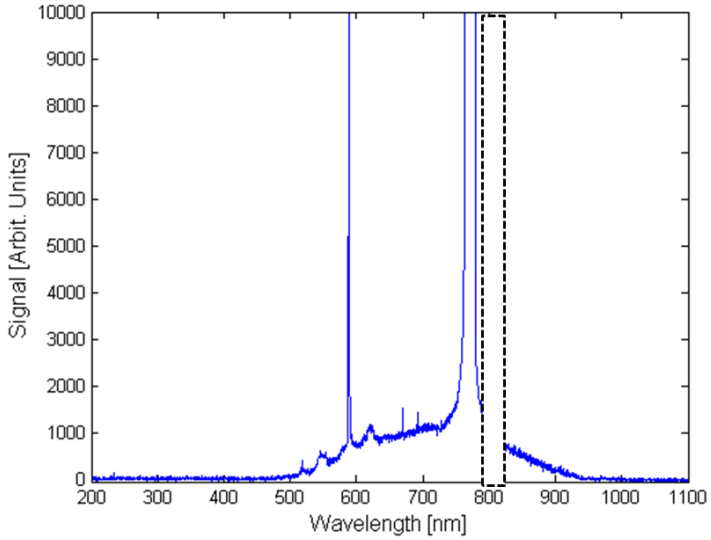

Figure 13: Emission spectra from Red Dot reaction recorded using Ocean Optics spectrometer.

The form factor of the Ocean Optics spectrometer and the wide frequency detection range makes the instrument well suited for field use. For this work spectral lines were identified during post-test data analysis. Real-time detection of heavy metals or other harmful emissions will be necessary for future field-ready system.

Light Extinction

Light extinction measurements were performed using the same input light source as the LII technique. The transmitted laser energy was detected using an integrating sphere and photodiode. Integrating spheres are used for total flux and irradiance measurements and consist of a hollow sphere coated with a material of greater than 98% reflectivity. The high reflectivity allows any part of the sphere surface to "see" all other parts of the sphere surface equally. A detector placed at any point on the sphere's surface can measure the total power in the entire sphere. The integrating sphere ensures all of the transmitted laser beam energy is detected without having to focus the high power laser directly onto the photodiode causing damage. Spheres are commercially available in various diameters which will be helpful for construction of a field-ready detection system.

For each reaction a series of high speed video images are shown below in addition to the corresponding light extinction measurements and thermocouple data. Light extinction data plots show the initiation trigger signal in blue and the photodiode signal in green. The black line on the plot is used to highlight the photodiode signal maxima resulting from the pulsed laser system. Each energetic material was initiated in the same manner described previously; 40 mg samples unconfined at atmospheric pressure using an electric match. The IM-68 reaction attenuated the greatest amount of laser signal, followed by $BKNO_3$, IM-23, and the Red Dot. Materials with more condensed phase products caused the most attenuation as expected. Results show that the fastest material reaction is complete in ~0.02 seconds indicating a data acquisition rate of 500 Hz should be sufficient for future measurements.

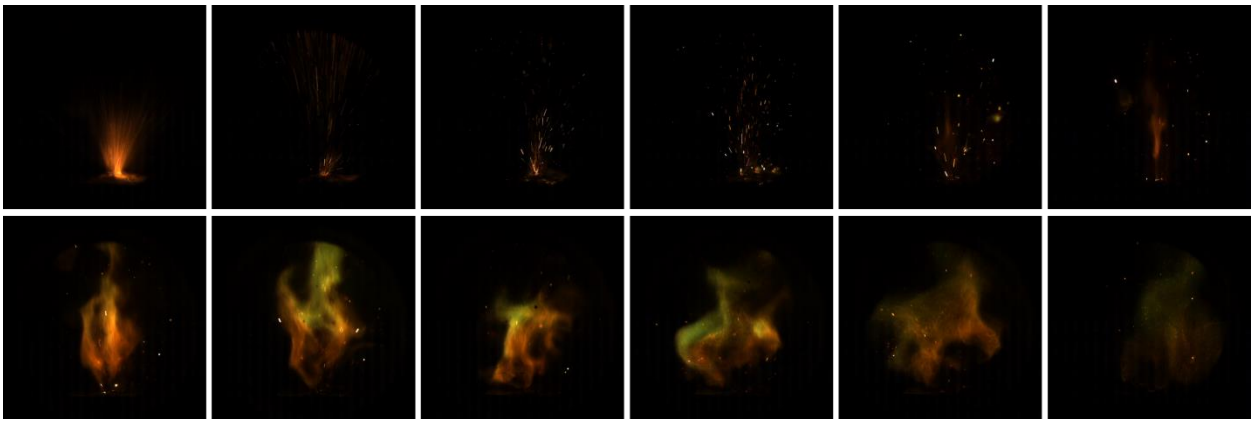

Figure 14: High speed camera image series of $BKNO_3$ reaction.

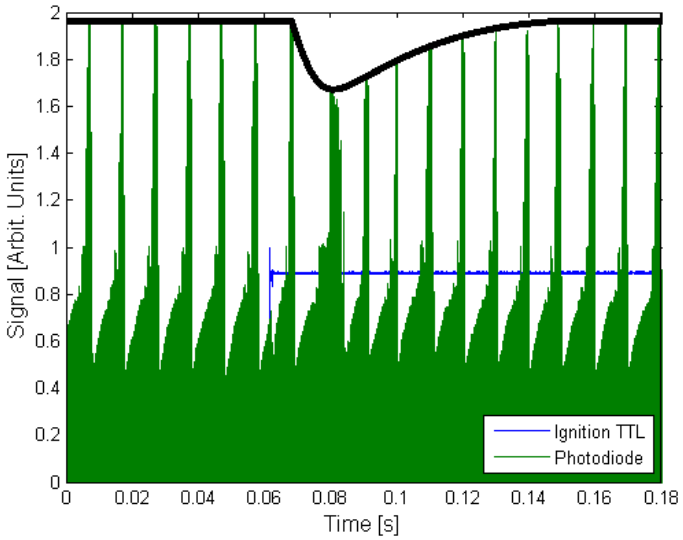

Figure 15: Light extinction measurement of $BKNO_3$ reaction.

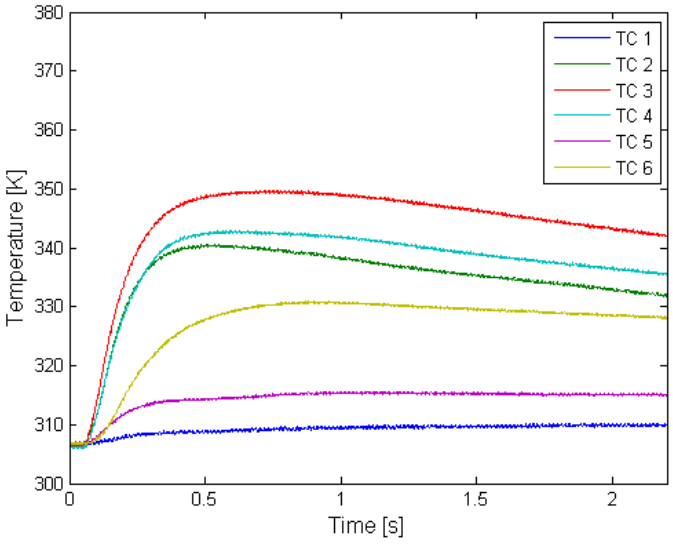

Figure 16: Thermocouple results for reaction of $BKNO_3$.

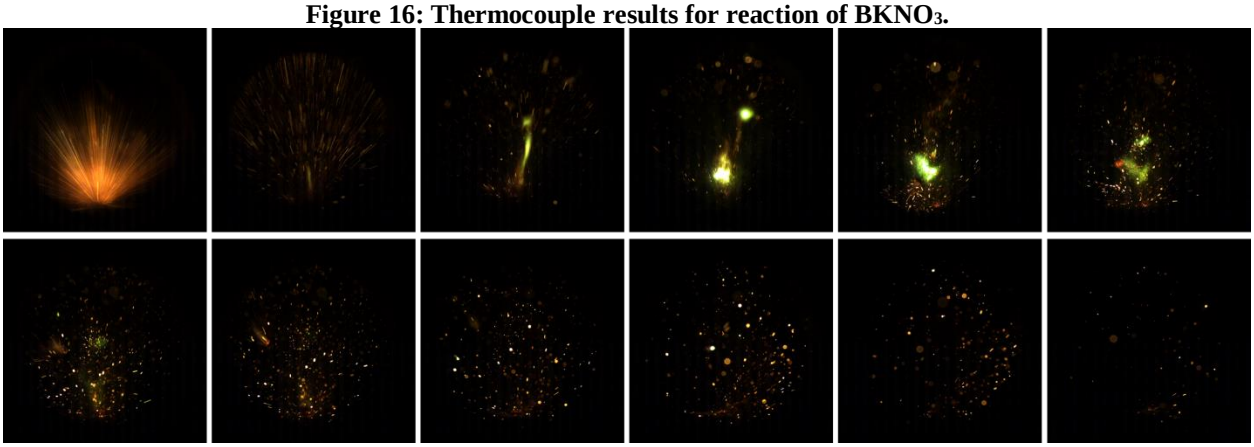

Figure 17: High speed camera image series of IM-23 reaction.

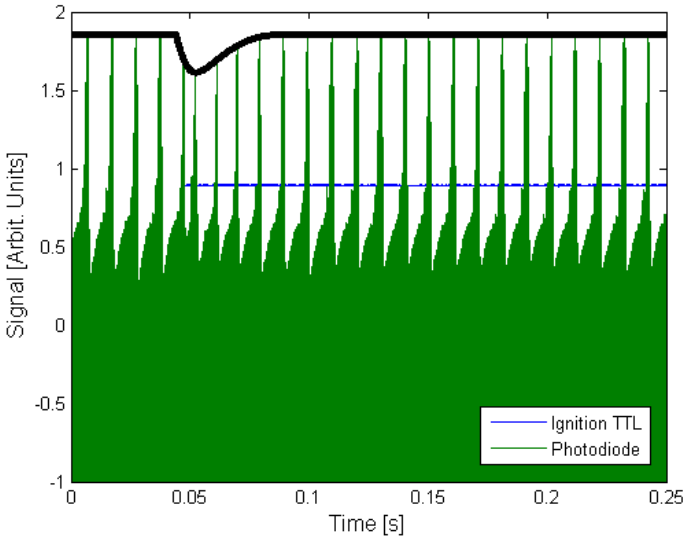

Figure 18: Light extinction measurement of IM-23 reaction.

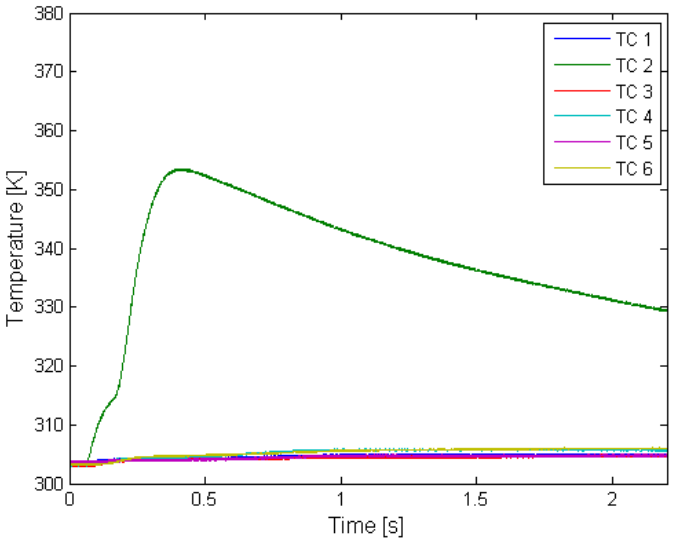

Figure 19: Thermocouple results for reaction of IM-23.

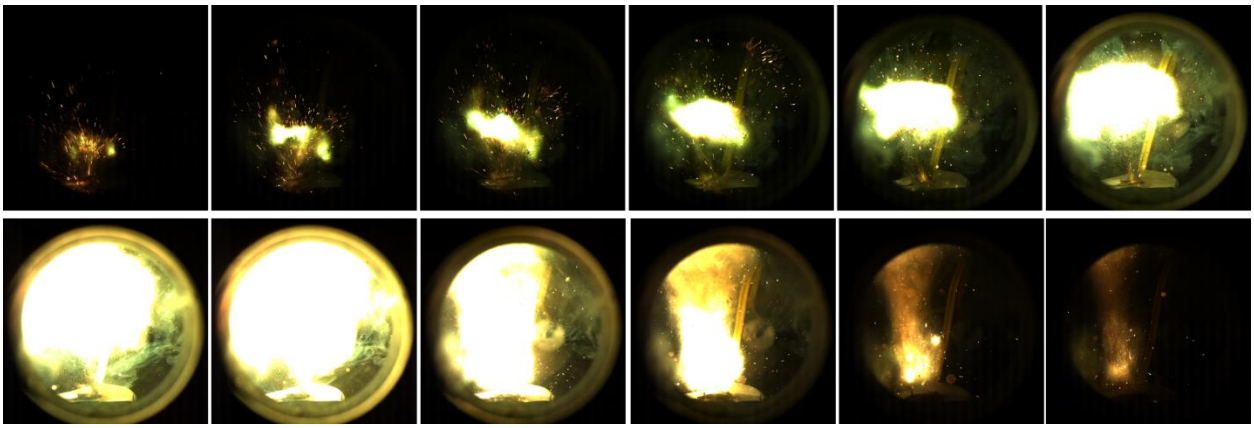

Figure 20: High speed camera image series of IM-68 reaction.

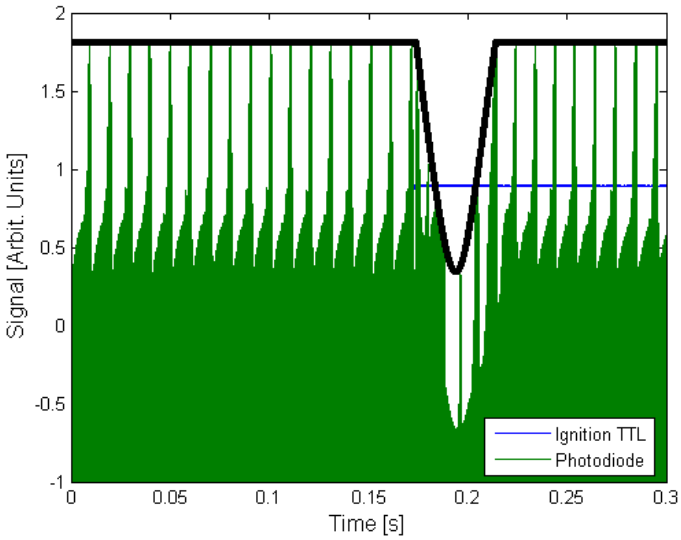

Figure 21: Light extinction measurement of IM-68 reaction.

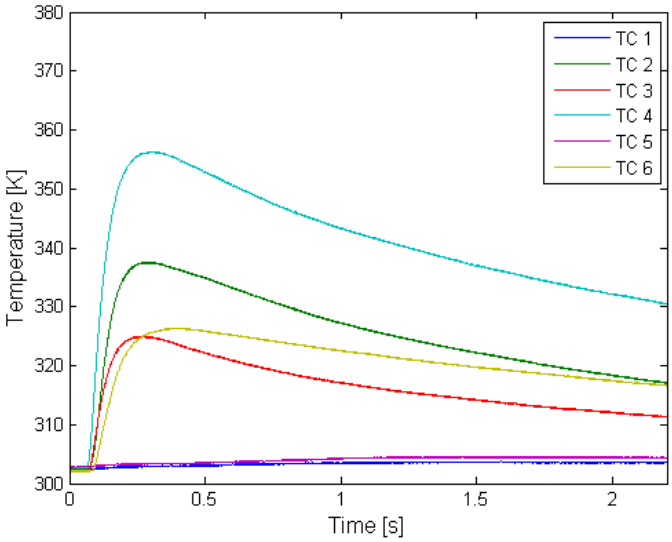

Figure 22: Thermocouple results for reaction of IM-68.

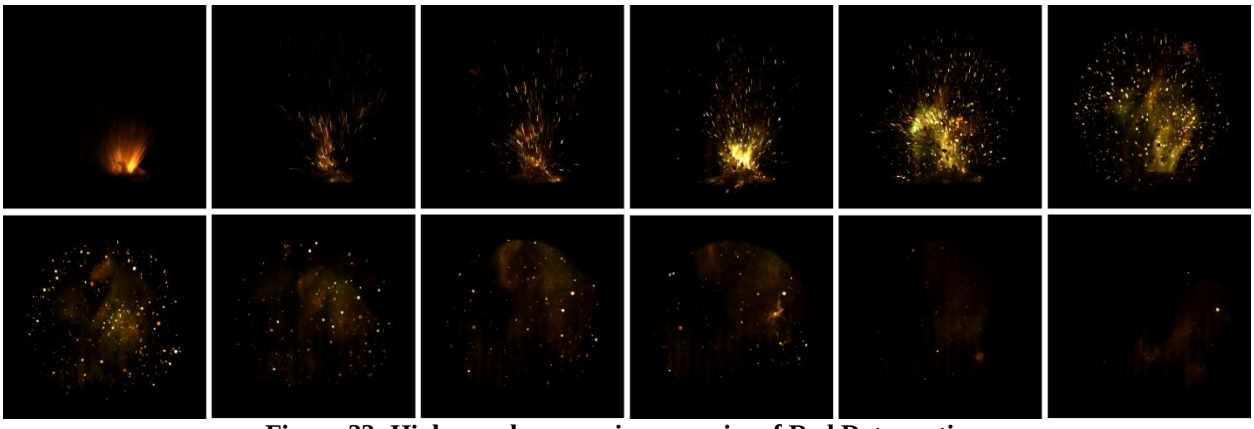

Figure 23: High speed camera image series of Red Dot reaction.

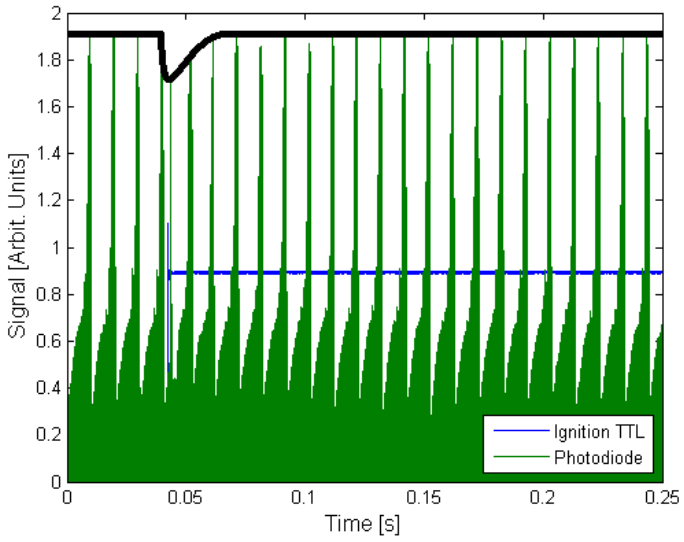

Figure 24: Light extinction measurement of Red Dot reaction.

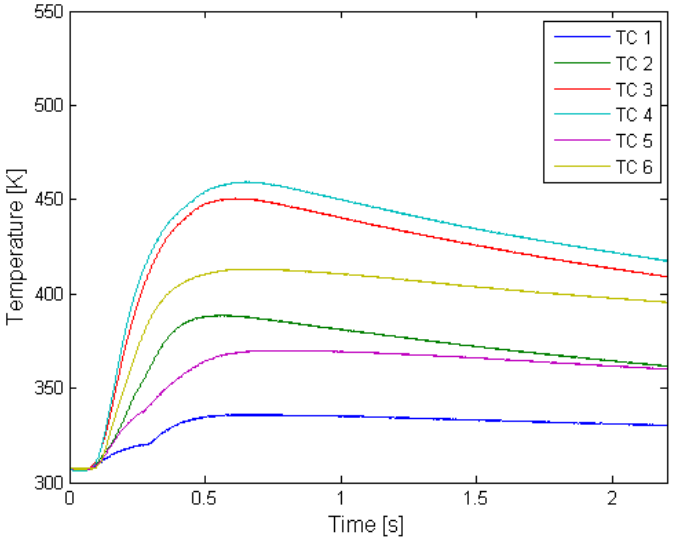

Figure 25: Thermocouple results for reaction of Red Dot.

Laser Induced Incandescence

For the laboratory proof-of-concept LII measurements a high power ultrafast laser system was used. The laser output power was much higher than needed for measurements; the beam was attenuated with a polarizer and wave plate to ~3 W. In addition, the ultrafast laser used is a highly sensitive instrument which must be operated in a temperature and humidity stable environment, not appropriate for field use. Commercial systems or appropriate output power and durability are available for future field-ready system integration.

The LII signal is generated by heating particles with a laser. Particles absorb the light and increase in temperature leading to a strong non-linear increase in thermal radiation, incandescence, in according to Planck's Law. Determination of particle size with pulsed laser LII is based on particle cooling rate after laser heating which results in a particle size dependent

decay rate of the LII signal that can be measured using time resolved detection, an example of this is shown in Figure 26.

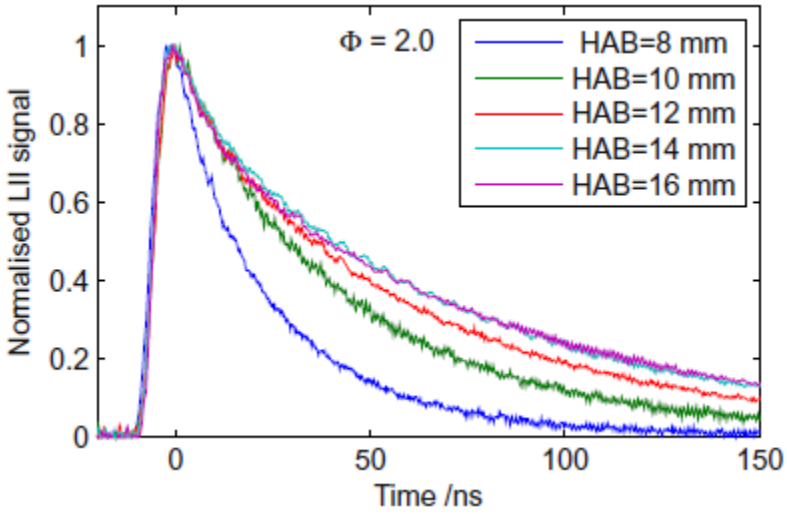

Figure 26: Example of LII signal decay for various particle sizes from Ref. 17.

With good experimental design and calibration LII measurements of volume and mass concentration can be made without a detailed heat transfer model, however this is required for accurate primary particle size determination[16]. Particle size is determined by comparison of pulsed LII signal decays with simulated ones based on the particle cooling rate and thermodynamics. These fundamental physical processes are accounted for in models such as LIISim which allows calculation of LII signal decay for variable experimental conditions.

The iCCD detector repetition rate was too slow to resolve the LII signal. This detector was selected for the gating capability; the integration time could be adjusted down to nanosecond timescales and for LII measurements fast gating is required to resolve the signal decay properly. The detector had the fast gating required but not the repetition rate. With a 5 kHz laser being used to generate the LII signal the detector should be able to operate at repetition rates above 20 kHz. Following these experiments the iCCD (Princeton Instruments PIMAX 3 1024i) was replaced with a highly sensitive high speed monochrome CMOS camera (Photron AX200 Mini). Results are shown in Figure 27.

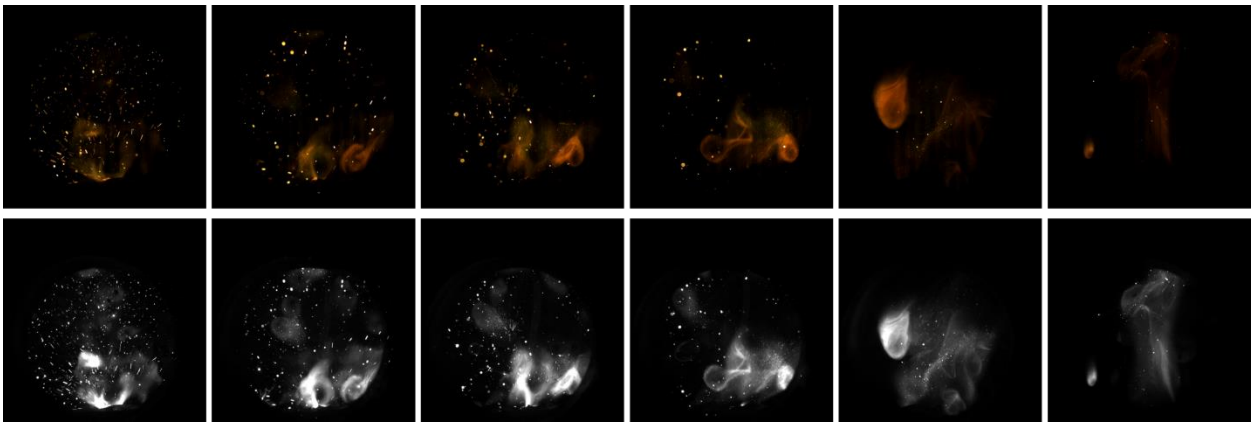

Figure 27: IM-68 reaction recorded with standard high speed camera (top) and by filtered laser scattering with monochrome high speed camera (bottom).

The CMOS camera was operated at the minimum possible exposure time, 260 ns. Due to the speed of the reactions this exposure time is an insufficient gating speed to resolve the LII signal decay and determine particle sizes. However it is clear from the recorded images that additional information is obtained when compared to the standard high speed video images. Figure 28 shows a high speed camera image and corresponding LII camera image. In the LII image fine smoke particles are visible which are not able to be detected by the high speed camera.

Figure 28: IM-68 reaction recorded with standard high speed camera (left) and by filtered laser scattering with monochrome high speed camera (right).

Commercially available array detectors at this time are insufficient for high repetition rate pulsed laser LII. A future field-use system should employ 1D LII measurements, if necessary at multiple locations, rather than 2D as single element detectors are available at the required speeds.

Cheetah Calculations

Lawrence Livermore National Laboratory's thermochemical code, CHEETAH Version 8.0, was used to determine the temperature and products of the energetic material reactions using constant volume (CV) calculations.

Table 2: Results from CHEETAH calculations.

Energetic Material	Product Composition [mole fraction]	Temperature [K]	Pressure [atm]
BKNO3	$B_{(l)}$ 0.5322 $B_{(s)}$ 0.1470 K 0.1069 B_2O_3 0.1069 BN 0.1069 Total Gas 2.162e-08 Total Condensed 1.0	2235.792	68412.405
Navy IM-23	MgO 0.4005 Al 0.2501 K 0.1704 Al_2O_3 0.09372 $MgCl_2$ 0.08521 Total Gas 4.722e-08 Total Condensed 1.0	5530.6	31324.28
Navy IM-68	H_2 0.1989 N_2 0.08394 NH_3 0.01364 H_2O 0.004741 H 0.004160 $Al_{(g)}$ 0.001041 $Ba_{(g)}$ 0.000177 N 6.239e-05 Mg 3.790e-05 NO 1.765e-05 MgO 0.3751 AlN 0.1160 $Al_{(l)}$ 0.1078 Al_2O_3 0.05654 $Ba_{(s)}$ 0.03471 Total Gas 0.3099 Total Condensed 0.6901	5026	46028.42
RedDot, NC-14	CO_2 0.2713 H_2O 0.2565 CO 0.2484 N_2 0.1463 NH_3 0.01321 CH_4 0.009101 H_2 ..... C_2H_4 0.002239 CH_3OH 7.541e-04	3224.9	111624.46

Energetic Material	Product Composition [mole fraction]	Temperature [K]	Pressure [atm]
	CH_2O_2 4.258e-04 C_2H_6 3.318e-04 C_2H_2 ..... Benzene 6.749e-05 NO 6.299e-05 C_3H_8 1.714e-05 C_2H_6O 1.168e-05 Acetone 5.649e-06 Total Gas 1.0 Total Condensed 2.232e-15		
RedDot, NC-1100	H_2O 0.2982 CO_2 0.2415 CO 0.1428 N_2 0.1060 NH_3 0.01718 CH_4 0.01675 H_2 ..... C_2H_4 0.002863 CH_3OH 0.00111 C_2H_6 9.991e-04 CH_2O_2 3.229e-04 Benzene 2.776e-04 C_2H_2 ..... C_3H_8 8.215e-05 C_2H_6O 2.225e-05 Acetone 1.406e-05 NO 1.059e-05 Graphite 0.1467 Total Gas 0.8533 Total Condensed 0.1467	2827.225	100070.77

CHEETAH has a multitude of different nitrocellulose versions to choose from. The Hercules RedDot material was run with two different versions of nitrocellulose (NC); versions with the lowest and highest nitrogen content. There is a significant difference in both temperature and species of the combustion products when different versions of NC are used. The exact version of NC used in the propellant is unknown and these results show potential variability in the formulation is significant.

There were many errors in calculations getting to the initial point for IM-68. The CV case was run after multiple initial points and the results were the same in every case, indicating errors in initial point value do not cause an inconsistency in the output.

CHEETAH calculations are consistent with spectroscopic measurement results.

Conclusions and Implications for Future Research

The goal of this project was to assess the use of optical diagnostic techniques for the standoff detection of hazardous combustion products produced from the reaction of energetic and pyrotechnic formulations. By performing laboratory scale testing for proof of concept data was for comparison with thermochemical calculations to provide insight towards the miniaturization and simplification of the diagnostic techniques for eventual application in a field-ready system.

A combustion chamber was instrumented with each diagnostic technique for simultaneous data acquisition during the reactions of BKNO3, Red Dot gun powder, Navy IM-23, and Navy IM-68. The laboratory proof-or-concept testing was successful, however several changes and improvements are recommended for future integration into a field-ready compact fiber optic-based system. Laser based techniques will need to be performed using a fiber-based diode laser. Several commercial products exist and it is recommended that an eye-safe center wavelength be chosen. Due to the availability and cost of high speed iCCD detectors it is recommended that LII measurements be performed as point measurements rather than attempting 2D spatially resolved measurements. Point measurements will also require less laser intensity for excitation. By using a photomultiplier tube or other highly sensitive small area detector appropriate temporal resolution can be achieved. As the field-use system will likely be used on a firing range outdoors, the fiber-based Ocean Optics spectrometer should be verified in bright daylight to account for possible interferences. A larger diameter fiber should be obtained for use with the spectrometer for better throughput in low signal conditions.

Development of a mobile and compact system, as an extensive follow-on project, may be used in the field to assess new technologies employed for reducing the long-term health effects associated with airborne metal emissions. One possible field-use system configuration is shown in Figure 29.

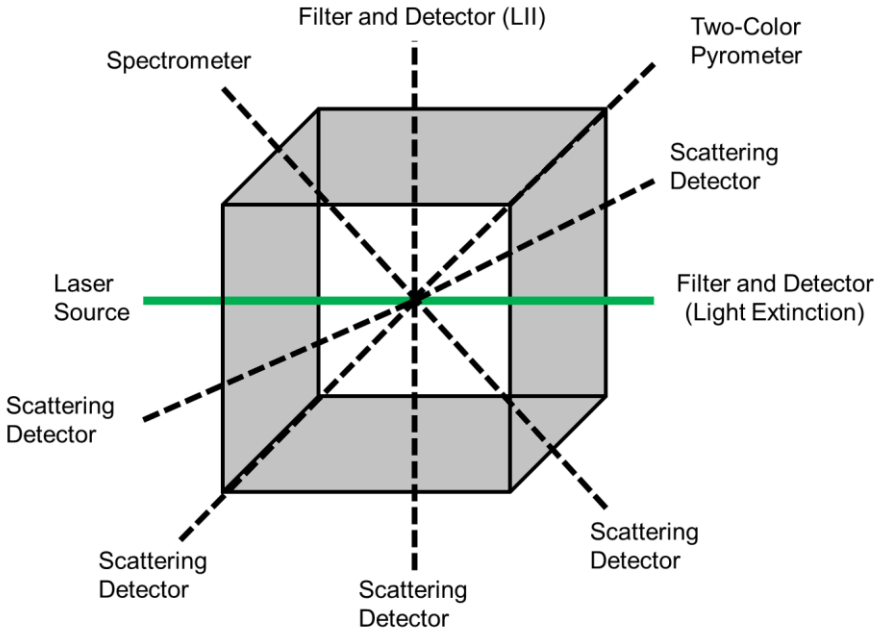

Figure 29: Schematic of configuration for future field-use system.

In addition to the diagnostic techniques investigated for this work another technique, Laser Induced Breakdown Spectroscopy (LIBS), may be especially useful for standoff metal species detection. This technique has already been demonstrated for explosives detection[18] and integrated in rugged field-use systems[19].

In order for such a device to be of practical use, measurements should be interpreted at or near real-time. The device should be designed with a computer controller running software capable of managing simultaneous data acquisition such as LabView in order to detect heavy metal species in the air. A spectroscopic library of airborne hazards and contaminants will need to be generated to compare with live spectroscopic results.

Literature Cited

1. Singh, J., Kalamdhad, A. S., "Assessment of bioavailability and leachability of heavy metals during rotary drum composting of green waste", *Ecological Engineering*, 2013; 52, 59.
2. Li, L., Xu, Z., Wu, J., Tian, G., "Bioaccumulation of heavy metals in the earthworm Eisenia fetida in relation to bioavailable metal concentrations in pig manure", *Bioresource Technology*, 2010; 101, 3430.
3. Steinhauser, G., Sterba, J. H., Foster, M., Grass, F., Bichler, M., "Heavy metals from pyrotechnics in New Years Eve snow", *Atmospheric Environment*, 2008; 42, 8616-8622.
4. Aduev, B. P., Aluker, E. D., Krechetov, A. G., Mitrofanov, A. Y., "Explosive Luminescence of Heavy Metal Azides", *Physica Status Solidi B*, 1998; 207, 535.
5. Aduev, B. P., et al., "Luminescence of lead azide induced by the electron accelerator pulse", *Journal of Luminescence*, 2000; 91, 41-48.
6. Grisch, F., et al., "Real time diagnostics of detonation products from lead azide using coherent anti-Stokes Raman scattering", *Applied Physics Letters*, 1991; 59, 27.
7. Crespo, J., et al., "High-time resolution and size-segregated elemental composition in high-intensity pyrotechnic exposures", *Journal of Hazardous Materials*, 2012; 241, 82-91.
8. Zhu, J., et al., "Measurement of light extinction constant of JP-8 soot in the visible and near-infrared spectrum", *International Journal of Heat and Mass Transfer*, 2004; 47, 3643.
9. Choi, M. Y., Mulholland, G. W., Hamins, A., Kashiwagi, T., "Comparisons of the Soot Volume Fraction Using Gravimetric and Light Extinction Techniques", *Combustion and Flame*, 1994; 102, 161-169.
10. Schulz, C., et al., "Laser-induced Incandescence: Recent Trends and Current Questions", *Appl. Phys. B*, 2006; 83, 3.
11. Snelling, D. R., Smallwood, G. J., Gulder, O. L., (1999). *U.S. Patent No. 6181419 B1*. Washington, DC: U.S. Patent and Trademark Office.
12. Wainner, R. T., Seitzman, J. M., "Soot Diagnostics Using Laser-induced Incandescence in Flames and Exhaust Flows", 37th AIAA ASM, 1999; AIAA 99-0640.
13. Ditaranto, M., Meraner, C., Haugen, N. E. L., Saanum, I., "Influence of long pulse duration on time-resolved laser-induced incandescence", *Appl. Phys. B.*, 2013; 113, 3.
14. Albro, R. A., Tran, T., Johnson, C., Fineman, C., "Optical Method for Fast Temperature Measurements," JANNAF 43rd Combustion/31st Airbreathing Propulsion/25th Propulsion Systems Hazards Joint Subcommittee Meeting, December 2009, La Jolla, CA
15. Itoh, T., Hashimoto, R., "Flourescense and nonradiative processes of dioxin vapors", *Spectrochimica Acta Part A*, 2014; 112, 158-163.
16. Michelsen, H. A., Schulz, C., Smallwood, G. J., Will, S., "Laser-induced incandescence: Particulate diagnostics for combustion, atmospheric, and industrial applications", *Prog. Energy Combust. Sci.*, 2015; 51, 2-48.
17. Bladh, H. Olofsson, N-E., Mouton, T., Simonsson, J., Mercier, X., Faccinetto, A., et al., "Probing the smallest soot particles in low-sooting premixed flames using laser induced incandescence", *Proc. Combust. Inst.*, 2015; 35, 1843.
18. Gottfried, J. L., De Lucia, F. C., Munson, C. A., Miziolek, A. W., "Laser-Induced Breakdown Spectroscopy for Detection of Explosives Residues: A Review of Recent Advances, Challenges, and Future Prospects", *Anal. Bioanal. Chem.*, 2009; 395, 283–300.

19. Moros, J., Lorenzo, J. A., Lucena, P., Tobaria, L. M., Laserna, J. J., “Simultaneous Raman Spectroscopy−Laser-Induced Breakdown Spectroscopy for Instant Standoff Analysis of Explosives Using a Mobile Integrated Sensor Platform”, *Anal. Chem.*, 2010; 82, 4.